Review of Scientific Instruments

Integration of a superconducting nanowire single-photon detector into a confocal microscope for time-resolved photoluminescence (TRPL)-mapping: Sensitivity and time resolution

Volker Buschmann (ID) ; Eugeny Ermilov ✉ (ID) ; Felix Koberling; Maria Loidolt-Krüger (ID) ; Jürgen Breitlow (ID) ; Hugo Kooiman (ID) ; Johannes W. N. Los; Jan van Willigen; Martin Caldarola (ID) ; Andreas Fognini (ID) ; Mario U. Castaneda; Jessica de Wild (ID) ; Bart Vermang (ID) ; Guy Brammertz (ID) ; Rainer Erdmann (ID)

Check for updates

CrossMark

View Online   Export Citation

AIP Publishing

Integration of a superconducting nanowire single-photon detector into a confocal microscope for time-resolved photoluminescence (TRPL)-mapping: Sensitivity and time resolution

View Online   Export Citation   CrossMark

Volker Buschmann,[1] 🆔 Eugeny Ermilov,[1,a)] 🆔 Felix Koberling,[1] Maria Loidolt-Krüger,[1] 🆔 Jürgen Breitlow,[1] 🆔 Hugo Kooiman,[2] 🆔 Johannes W. N. Los,[2] Jan van Willigen,[2] Martin Caldarola,[2] 🆔 Andreas Fognini,[2] 🆔 Mario U. Castaneda,[2] Jessica de Wild,[3,4,5] 🆔 Bart Vermang,[3,4,5] Guy Brammertz,[3,4,5] 🆔 and Rainer Erdmann[1] 🆔

AFFILIATIONS

[1] PicoQuant GmbH, Rudower Chaussee 29, D-12489 Berlin, Germany
[2] Single Quantum, Rotterdamseweg 394, 2629 HH Delft, The Netherlands, info@singlequantum.com
[3] Hasselt University, Imo-Imomec, Martelarenlaan 42, 3500 Hasselt, Belgium
[4] Imec, Imo-Imomec, Thor Park 8320, 3600 Genk, Belgium
[5] EnergyVille, Imo-Imomec, Thor Park 8320, 3600 Genk, Belgium

[a)]Author to whom correspondence should be addressed: ermilov@picoquant.com

ABSTRACT

This report highlights the combination of the MicroTime 100 upright confocal fluorescence lifetime microscope with a Single Quantum Eos Superconducting Nanowire Single-Photon Detector (SNSPD) system as a powerful tool for photophysical research and applications. We focus on an application in materials science, photoluminescence imaging, and lifetime characterization of $Cu(InGa)Se_2$ (CIGS) devices intended for solar cells. We demonstrate improved sensitivity, signal-to-noise ratio, and time-resolution in combination with confocal spatial resolution in the near-infrared (NIR) range, specifically in the 1000–1300 nm range. The MicroTime 100–Single Quantum Eos system shows two orders of magnitude higher signal-to-noise ratio for CIGS devices' photoluminescence imaging compared to a standard NIR-photomultiplier tube (NIR-PMT) and a three-fold improvement in time resolution, which is now limited by the laser pulse width. Our results demonstrate the advantages in terms of image quality and time resolution of SNSPDs technology for imaging in materials science.

I. INTRODUCTION

Over the years, luminescence spectroscopy has become one of the fundamental methods for analyzing the photophysical properties of a variety of samples, ranging from organic molecules to semiconductor materials and photovoltaic (PV) devices. It is worth emphasizing that detection sensitivity is a key parameter to meet today's demands for handling weakly luminescent samples and for short measurement times in the optical evaluation of, for example, PV devices. The introduction of single-photon counting based data acquisition has proven to yield a major sensitivity increase and very

high dynamic range[1]—it is the ideal method for measuring weak photoluminescence (PL).

The commonly used steady-state luminescence spectroscopy methods provide valuable insights into the photophysics of a sample. However, such results give only a partial view of the sample's behavior after photoexcitation. A further piece of the puzzle is often revealed by performing time-resolved luminescence spectroscopy, as it provides deeper insights into the photophysical processes occurring in the sample under investigation. An even more comprehensive picture is gained by including spatial information.[2] Acquiring time-resolved spectroscopic data at regions of interest (ROIs) of

04 July 2023 14:13:16

the sample can help in inferring structural-to-photophysical relationships in different materials and can give information about important photophysical processes as well as changes in the local environment of emitting species. For example, fluorescence lifetime imaging microscopy is a very well established imaging method in life sciences, where the lifetime information is combined with spatial localization in the sample, allowing investigating of biochemical or physical processes, or probing the local environment of the fluorophore.[3] As processes commonly investigated in materials science are mostly not classical fluorescence processes, in general, the term time-resolved photoluminescence (TRPL) imaging is more adequate. In materials science, TRPL imaging can be used for the characterization of key parameters, such as, e.g., charge carrier dynamics and mobility in semiconductors.[4] It is worth mentioning that very often these processes occur on timescales ranging from tens of picoseconds to several hundreds of nanoseconds.[5]

In order to achieve high temporal resolution, high repetition rate lasers with short pulses, and detectors with a fast response function, along with appropriate time-correlated single-photon counting (TCSPC) electronics have to be used.[6] For the UV–Vis spectral range (200–900 nm), there are fast and sensitive single-photon counting detectors with low dark noise [e.g., PMA Hybrid detectors from PicoQuant, with quantum efficiency up to 40%, dark noise <200 counts/s, as well as timing resolution down to <50 ps full-width half maximum (FWHM)], whereas for the near-infrared (NIR) spectral range (900–1500 nm), the choice of suitable detectors is very limited. Traditional photomultiplier tubes (PMTs) operating in the NIR spectral range show significant limitations related to their detector performance, such as low quantum efficiency (typically 2–5%), high dark noise level (depending on the detector type, up to 200 000 counts/s), and moderate timing resolution [(≤300 ps (FWHM)].

In terms of detector performance, superconducting nanowire single-photon detectors (SNSPDs) stand out due to achievable close-to-unity detection efficiency in NIR spectral range,[7,8] picosecond timing resolution [down to <20 ps (FWHM)[9,10]], and low dark noise (<100 counts/s).[7] The nanowires in this work were fabricated from NbTiN thin films. The dark-counts are very low for the fiber coupled SNSPD systems for two reasons. First, the sensor is cooled to about 2.5 K, which keeps the intrinsically generated black body radiation within the cryostat at a minimum. Second, the detectors used in this work have only a significant efficiency below 1500 nm where the black-body radiation coupled to the optical fiber from the outside of the cryostat is estimated to be <100 counts/s. The response time of an SNSPD is very fast because the inelastic electron–electron scattering in the superconductor happens on the order of a few picoseconds.[11]

SNSPDs are a rather new technology that is being used in multiple applications in the fields of quantum optics, luminescence lifetime measurements, and singlet oxygen detection, just to mention a few.[7] The high sensitivity due to high quantum efficiency combined with the low dark count rate is especially important for materials science applications in the NIR-range beyond 1000 nm, where, as discussed above, other available single-photon counting detectors have a low detection efficiency, high dark count rate, and slow response time.[12]

In this report, we demonstrate the combination of the Micro-Time 100 upright confocal fluorescence lifetime microscope with the Single Quantum Eos SNSPDs as a powerful tool for photophys-

ical research, especially in the materials science, yielding spatial and temporal information on semiconductor samples studied through PL emission.

II. SYSTEM INTEGRATION: MICROTIME 100–SNSPD COUPLING

The measurement setup as shown in Fig. 1 was a MicroTime 100 confocal microscope (PicoQuant, Germany) in combination with a Single Quantum Eos SNSPD system. For excitation, we used a pulsed diode laser (LDH-P-C-640, PicoQuant) emitting at 640 nm fiber-coupled to the MicroTime 100. The excitation light was focused on a diffraction-limited spot on the sample by a 20× LC Plan NIR-optimized objective (Olympus). Emitted luminescence was collected through the same objective, and an image was constructed by raster scanning the microscope objective. A 1000 nm longpass filter (Edmund Optics) was used to remove any excitation light in combination with a 780 nm longpass filter (AHF). The second filter was necessary to completely remove excitation light due to the high scattering and reflection of the solid-state samples used. Then, the emitted luminescence was coupled into a multi-mode fiber with a 50 μm diameter (Thorlabs), which served as a confocal pinhole. This fiber was used to deliver light to the Single Quantum Eos system or to the FluoTime 250, as depicted in Fig. 1.

For comparative measurements with a standard NIR-PMT, the collected PL was fed into a FluoTime 250 spectrometer[13] equipped with a NIR-PMT (H10330-45, Hamamatsu) using the 50 μm multi-mode fiber. In order to avoid any additional losses of the luminescence signal, the emission polarizer of the spectrometer was removed from the beam path, the emission attenuator was fully opened, and the same emission filters as for measurements with the SNSPD system were used. No monochromator was present in the system. We have chosen the FluoTime 250 spectrometer since it contains all the necessary electronics and optics for coupling the NIR-PMT as well as the optical fiber.

The SNSPDs were part of a Single Quantum Eos system (from Single Quantum, The Netherlands). The left side of Fig. 2 shows a picture of the system, including driving electronics and the cold head with the FC/PC input fiber ports (eight-channel system in the picture). On the right, we show an SEM micrograph of the superconducting nanowire with a diameter of ~16 μm.

For measurements with these detectors, we coupled the confocal fiber directly to the internal fibers of the SNSPD-detection unit. Several sensors were present in the system, each sensor used a separate internal fiber to deliver the light from an external fiber connector. The Single Quantum Eos system had FC–PC connectors to transfer the emission from the external 50 μm multi-mode fiber from the MicroTime 100 to the internal fibers connected to the sensors. We compare two different SNSPD designs: one designed for single-mode fibers and another one for multi-mode fibers. The single-mode SNSPD had a diameter of 16 μm with a peak detection efficiency of around 900 nm, and the internal fiber had a 9 μm core diameter (SMF-28). The larger multi-mode SNSPD had a diameter of 25 μm with a peak detection efficiency of around 1064 nm, and the internal fiber used was a custom-made 28 μm-core diameter graded index multi-mode fiber. We used this internal custom-made fiber and not a standard 50 μm multi-mode fiber to closely match the detector size with the fiber core diameter, thus improving the
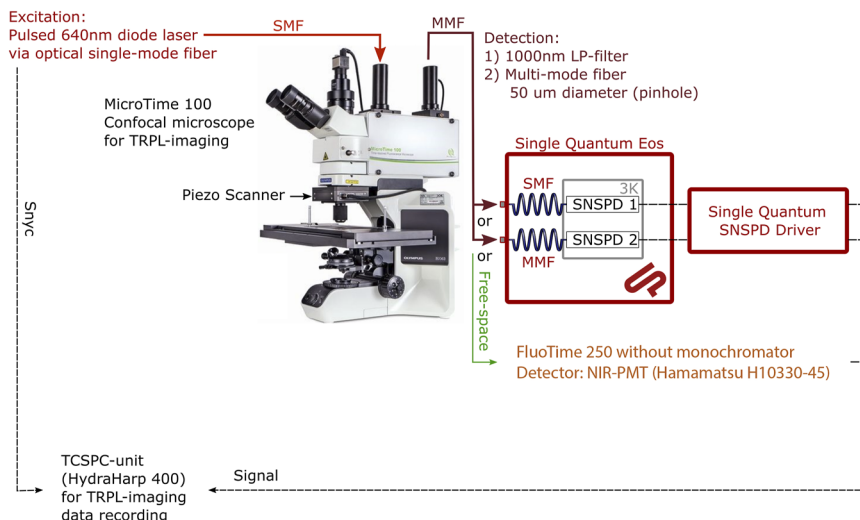
04 July 2023 14:13:16

FIG. 1. Experimental setup. The MicroTime 100 confocal microscope is combined with the Single Quantum Eos for TRPL imaging. We use a 640 nm pulsed laser diode as an excitation source that is fed to the microscope using a polarization maintaining single-mode fiber (SMF). The light is focused on the sample by a microscope objective that also collects the emitted photoluminescence. To build an image, the sample is spatially scanned by a piezo 2D scanner (PI). We use a multi-mode fiber (MMF) of 50 μm core diameter as a confocal "pinhole," and to deliver the emitted light to different detectors, we choose between a single-mode and a multi-mode SNSPD from Single Quantum (accessed with single-mode or multi-mode fibers, respectively), or a FluoTime 250 lifetime spectrometer from PicoQuant to measure with a NIR-PMT (Hamamatsu). The HydraHarp 400 TCSPC module allows TRPL measurements from electrical pulses created by the SNSPDs or the NIR-PMT.

system performance in terms of high count rates and reduced dark counts.

In order to detect light using an SNSPD, we need to apply a bias current that flows with no resistance through the superconducting nanowire, often called the bias current. When a photon is absorbed, it stops the zero-resistance flow (it breaks the superconducting state),[7,15,16] and the nanowire responds as a normal non-superconducting metal for some time. In this situation, the current now flows toward an amplifier that creates the electrical pulse that indicates a photon-detection event. After a recovery time of a few 10 ns, the superconducting state is restored, and the detector is ready for a new detection event.
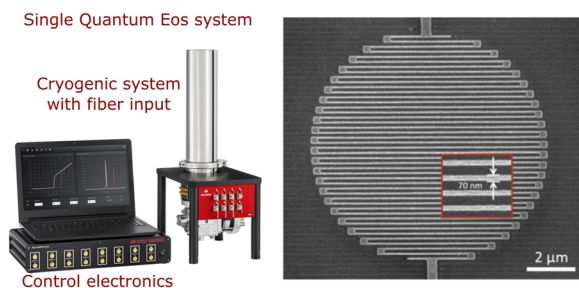

FIG. 2. Single Quantum Eos superconducting single photon detection system.[14] Left: complete system with fiber coupled detectors, amplification, and control electronics with the proprietary software interface. Right: Scanning electron micrograph of a superconducting nanowire single photon detector, inset: details of the superconducting nanowire featuring a width of 70 nm.

It is important to note that the SNSPD detection efficiency strongly depends on the chosen bias current value. Therefore, a fixed bias current is needed for SNSPD operation, called the operating current. Figure 3 depicts the measured detection efficiency as a function of the bias current as well as the measured dark counts for the two detectors used in this paper, for the multi-mode detector [Fig. 3(a)], and for the single-mode detector [Fig. 3(c)]. Note that the dark counts are higher for the multi-mode case caused by the higher chance of coupling black-body radiation into the detector through the larger core diameter of the fiber and the larger diameter of the detector. We also depict a plot of the wavelength dependence of the efficiency for these SNSPDs [Figs. 3(b) and 3(d)]. We emphasize here that by design, these detectors are narrow-band and made for a working wavelength of 1064 nm for the multi-mode detector and 900 nm for the single-mode detector. This condition can be relaxed, and broadband SNSPDs detectors can be fabricated as well as custom-made requirements that can be combined in different spectral channels, each recorded by a different SNSPD.

For all detectors, the electrical signal output was connected to a HydraHarp 400 single-photon counting unit to record the time-resolved data. Imaging of areas up to $80 \times 80 \ \mu m^2$ was achieved by objective scanning via a piezo scanner, and that of larger areas was achieved by raster-scanning of the sample using a wide-range-scanner. Images were collected and analyzed using the microscope system's SymPhoTime64 software.

An important characterization parameter for a TCSPC microscope is the so-called instrument response function (IRF), which provides information regarding the timing resolution of the system when using the time-tagging mode. We take the timing resolution of
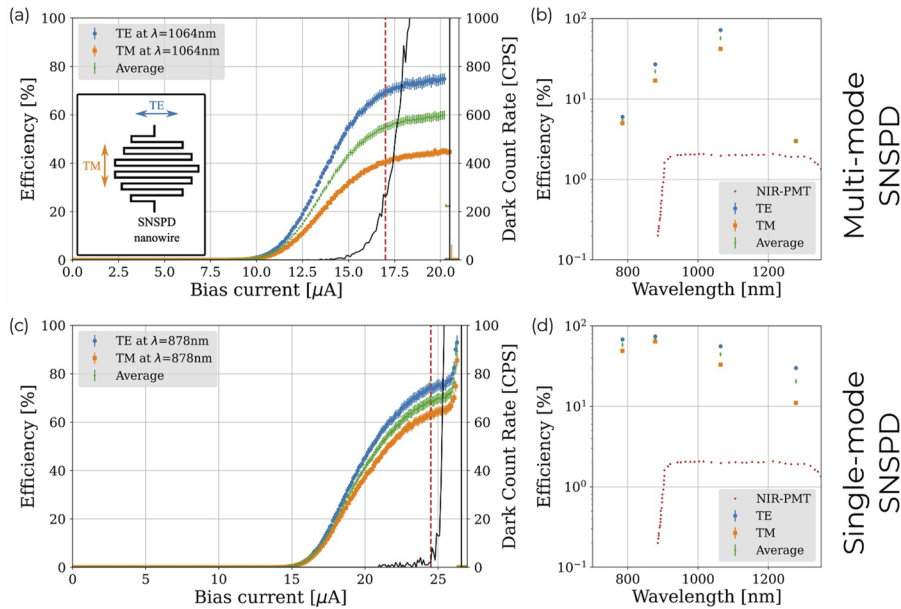
FIG. 3. SNSPD characterization. System detection efficiency for different bias currents for multi-mode (a) and single-mode (c) SNSPDs, measured at the indicated wavelength and polarization state [transverse electric (TE) and transverse magnetic (TM), correspondingly]. The right vertical axis depicts the measured dark counts (solid black curves), and the vertical dashed lines indicate the operating current. The inset in (a) depicts the polarization direction for the TE and TM modes with respect to the SNSPD meander. On the right panels, we show the wavelength dependence of the efficiency for multi-mode (b) and single-mode (d) SNSPDs in comparison with the NIR-PMT.

the system as the full-width half maximum (FWHM) of the IRF of the overall setup. In order to measure the IRF, we recorded the luminescence of the NIR emitting dye 3274y[17] with an emission peak at 1070 nm and with a previously reported lifetime below 10 ps[18] (which is significantly lower than the time resolution of our system). With this procedure, we obtained IRFs of 90 ps FWHM for the single-mode SNSPD, 120 ps for the multi-mode SNSPD, and 280 ps for the NIR-PMT, respectively. While the detector transit time spread (jitter) is the main limitation for the IRF for the case of the NIR-PMT, the jitter value for the SNSPDs (21 and 52 ps) is significantly smaller than the determined IRF, so we attribute the measured values to the actual pulse width of the excitation laser.

III. APPLICATION EXAMPLES

A. PL imaging of a CIGS device: Sensitivity study

In order to compare the sensitivity of SNSPDs with the traditional NIR-PMT (H10330-45, Hamamatsu), TRPL images of a $Cu(In,Ga)Se_2$ (CIGS)-based solar cell were recorded with the MicroTime 100 confocal microscope.

The solar cell was built up as a stack starting with a Molybdenum back contact, followed by a 1.5 μm thick CIGS layer, a 50 nm CdS buffer layer, a 150 nm intrinsic zinc oxide (iZnO) layer, and topped off with a 300 nm thick indium tin oxide (ITO) contact. A silver grid was layered over the top contact.[2] Luminescence emission of the sample is centered around 1260 nm [with a total half width of ~100 nm, see Fig. 4(d)], and emission was excited with the 640 nm pulse laser at 2 μW average power with a 20 MHz repetition rate.

For comparison, we have also measured the luminescence of the sample with the traditional Hamamatsu NIR-PMT mounted to the FluoTime 250 spectrometer. Longpass filters, excitation laser,

and TCSPC electronics were the same as for measurements with the SNSPD system.

All detectors were suitable for the measurements; however, we observed some striking differences in the brightness of the obtained images, as depicted in Fig. 4. With a measurement time per pixel of 2 ms, only around 10–30 photons/pixel could be collected in the bright areas when the combination of the MicroTime 100 and the NIR-PMT was used [Fig. 4(a), left]. By using the single-mode (SMF-28) fiber coupled SNSPD, the brightness increased significantly [around 200 to 800 photons/pixel could be collected, see Fig. 4(a), middle]. This proves that the high quantum efficiency of the SNSPD significantly overcompensates the probable losses due to the butt-coupling of the MicroTime's 50 μm detection fiber to the single-mode fiber of the SNSPD system. It involves a mismatch of core sizes from 50 to 9 μm, thus we expect some coupling losses. When using the multi-mode SNSPD, we measured a further increase of the brightness to around 1000–4000 photons/pixel [Fig. 4(a), right]. Given that the collection time/pixel is 2 ms, this corresponds to a 0.5–2 Mcps photon detection rate. From the presented results, it is evident that the SNSPDs provide images with a much superior brightness compared to the standard NIR-PMT detector, especially the multi-mode fiber connected version.

However, the brightness itself is not the only parameter of interest. For a classical TRPL analysis, the signal-to-noise (S/N) ratio is also important. As the noise levels of the three detector types are also quite different, we take the S/N as a fair metric to evaluate the detector's performance. We took a ROI in the image with a relatively homogeneous intensity and added the photons from this region to a TCSPC histogram. As for the S/N ratio, we checked here the ratio of the height of the peak divided by the noise showed as a lower baseline in the histogram. For the NIR-PMT, we got an S/N ratio of ~56, whereas for the single-mode and the multi-mode SNSPDs, the corresponding value was estimated to be ~24 000 and ~15 000,
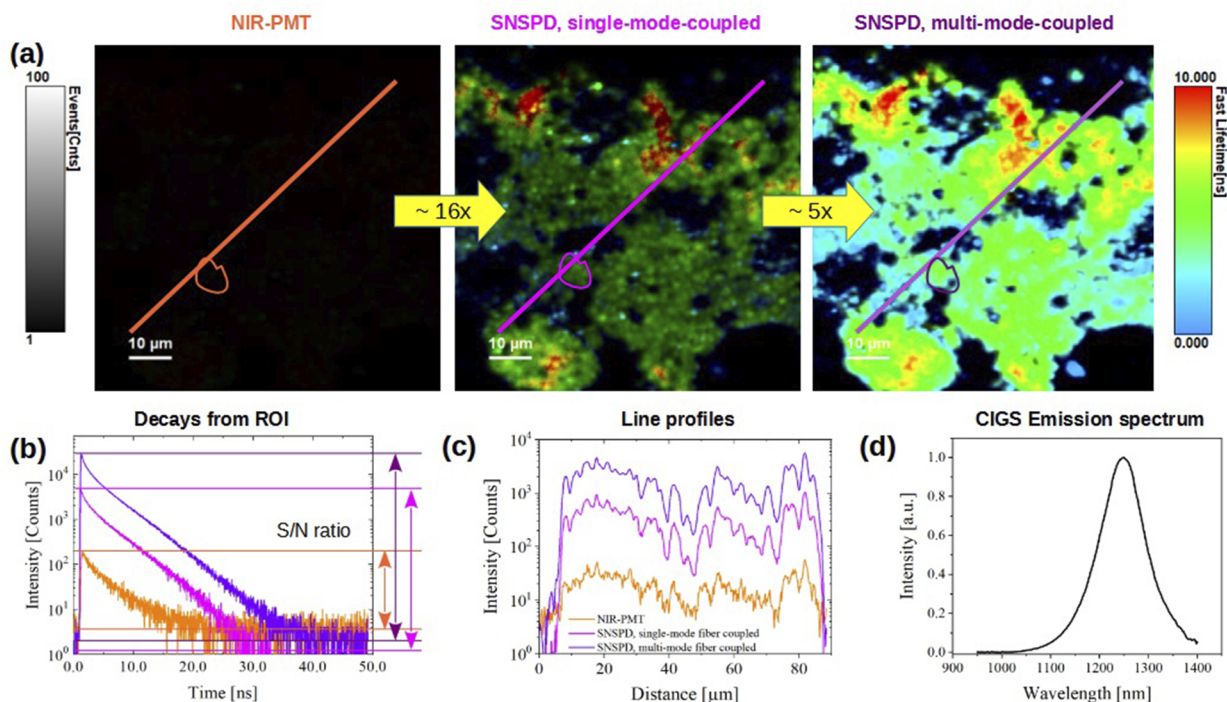
04 July 2023 14:13:16

FIG. 4. Detector comparison: brightness and lifetime S/N ratio. Intensity and TRPL images (a) for NIR-PMT (left), single-mode SNSPD (center), and multi-mode SNSPD (right). The lines in these images show the ROIs used to build the PL TCSPC histograms depicted in (b) and intensity line profiles (c) of the CIGS sample. (d) The emission spectrum of the CIGS sample.

respectively. Clearly, the SNSPDs beat the NIR-PMT detector in terms of S/N ratio by more than two orders of magnitude. Surprisingly, the S/N ratio among the two tested SNSPD types is in favor of the single-mode fiber coupled device. In Fig. 4(a), we see that ~5 times more light is detected with a multi-mode coupled SNSPD compared to a single-mode coupled SNSPD. However, considering the dark-counts presented in Fig. 3, we can see that for a single-mode coupled SNSPD, the dark-counts are <10 counts/s, whereas for a multi-mode coupled device, the dark-counts are >200 counts/s at their ideal operational point. This explains the better S/N for the single-mode fiber coupled device even though it couples less light but outperforms the multi-mode SNSPD in terms of dark-counts.

Overall, if we take into account the shorter dead-time, the better timing resolution, and the lower dark count rate of single-mode compared to multi-mode SNSPDs, the single-mode SNSPD is preferable in TRPL microscopy even though less PL signal is coupled to the sensor. This last point could be mitigated by using some specially tapered fibers or free-space optics to adapt the modes on the multi-mode fiber into the core of the single-mode fiber. Detailed measurements on this matter are needed to further optimize the combination of parameters.

B. TRPL-imaging of a weakly luminescent CIGS semiconductor device

We further tested our MicroTime 100 equipped with the SNSPDs detection unit by probing the photophysics of different semiconductor materials. Naturally, the presented increased count rates become more important in the case of weakly emitting samples.

In this example, the TRPL images were taken from the specially prepared thin-film CIGS sample.[19] The Cu(In, Ga)Se$_2$ absorber layers were grown on 1 mm Mo/SLG [sodalime glass] glass substrate using a single stage co-evaporation process. The substrate temperature was 550 °C. The layer thickness was 500 nm, and the Cu/(In + Ga) and Ga/(In + Ga) ratios were 0.8 and 0.3, respectively, derived from x-ray fluorescence measurements. The sample underwent a potassium fluoride (KF) treatment by spin coating a 0.2M KF solution in air and annealing the sample in a N$_2$ atmosphere for 20 min at 400 °C.[19] After annealing, the sample was covered with ~30 nm CdS deposited by chemical bath deposition.

We excited the photoluminescence of this sample using a pulsed laser at 640 nm with a 40 MHz repetition rate and a power of 17 μW at the sample, taking 300 × 300 px TRPL images with 5 ms measurement time per pixel. Then, we parked the laser at a point of interest in the sample and performed a single point measurement (PL decay curves) acquiring photons for 30 s.

Figure 5 depicts TRPL images as well as decay profiles that were taken at two different ROIs of the sample, namely at a point with quenched luminescence [defect side, blue curves in Figs. 5(c) and 5(d)] and at a point with high luminescence intensity (red curves in the corresponding figures). The PL intensity at defect sides is quenched due to localized defects in the CIGS layer, which then also results in faster decay for these areas. It is clearly seen that the combination of the MicroTime 100 microscope and the SNSPD
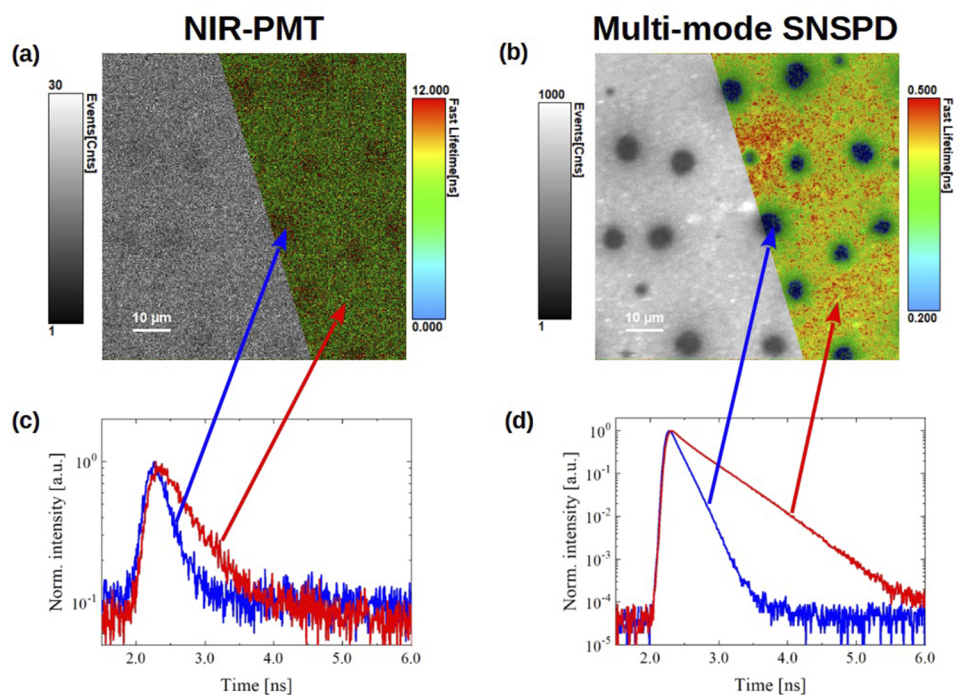
FIG. 5. TRPL images of weakly emitting CIGS. The intensity and time-resolved images (a) and (b) and PL decays acquired at two different ROIs of samples (c) and (d) measured with the NIR-PMT (a) and (c) and the multi-mode fiber coupled SNSPD (b) and (d).

allows for much better identification of the PL topology of the sample compared to the MicroTime 100 and NIR-PMT combination [see Figs. 5(a) and 5(b)]. Moreover, the very high sensitivity of the SNSPD even reveals clearly the differences in the PL decay profiles of the defect and unquenched areas of the sample, which is difficult to resolve when using the NIR-PMT detector. This result is not surprising if one takes into account that the S/N ratio in the measured decays was >10 000:1 for the SNSPD, whereas it is only 10:1 for the NIR-PMT sensor. This example highlights that the SNSPD in combination with the MicroTime 100 confocal system is capable of providing deeper insights into the relationships between structure and photophysical behavior even for very weakly luminescent samples. It should be emphasized that this information is hardly available when the PL of such a sample is detected with a conventional NIR-PMT.

IV. SUMMARY

We showed that a substantial increase in sensitivity is achieved by coupling the MicroTime 100 microscope to a Single Quantum Eos SNSPD when compared to a standard NIR-PMT detector. The recorded PL signal was increased by more than an order of magnitude by using the SNSPDs, and more importantly, the S/N ratio in TRPL measurements was improved by more than two orders of magnitude compared to the NIR-PMT detector.

In addition, we empirically compared single-mode and multi-mode SNSPD imaging capabilities. Obviously, the multi-mode coupled detector provided a better coupling of the PL signal. And yet, taking into account the benefits of a single-mode SNSPD like lower dark-counts, better time resolution, and shorter dead-time, it becomes evident that a single-mode SNSPD is the better choice for

the presented instrument combination between the MicroTime 100 and a Single Quantum Eos SNSPD system.

The combined systems allowed for the TRPL imaging of very weakly emitting materials, which can greatly reduce the time required for photophysical material analysis and significantly improve the quality of the results.

As an outlook, we envision a finely tuned SNSPD design to increase further the S/N ratio and the timing resolution for TRPL.

AUTHOR DECLARATIONS

Conflict of Interest

V.B., E.E., F.K., M.-L.-K., J.B., and R.E. are employed by PicoQuant and may profit financially. H.K., J.W. N.L., J.W., M.C., A.F., and M.U.C. are employed by Single Quantum and may profit financially. J.de.W., B.V., and G.B. have no conflicts to disclose.

Author Contributions

Volker Buschmann: Conceptualization (equal); Formal analysis (equal); Investigation (equal); Writing – original draft (equal); Writing – review & editing (equal). **Eugeny Ermilov**: Conceptualization (equal); Formal analysis (equal); Investigation (equal);

04 July 2023 14:13:16

Writing – original draft (equal); Writing – review & editing (equal). **Felix Koberling**: Project administration (equal); Writing – review & editing (equal). **Maria Loidolt-Krüger**: Resources (equal); Writing – review & editing (equal). **Jürgen Breitlow**: Funding acquisition (equal); Project administration (lead); Resources (lead); Supervision (lead); Writing – review & editing (equal). **Hugo Kooiman**: Conceptualization (equal); Formal analysis (equal); Investigation (equal); Resources (lead); Writing – original draft (equal); Writing – review & editing (equal). **Johannes W. N. Los**: Conceptualization (equal); Formal analysis (equal); Investigation (equal); Writing – original draft (lead); Writing – review & editing (equal). **Jan van Willigen**: Project administration (equal). **Martin Caldarola**: Funding acquisition (equal); Project administration (equal); Supervision (equal); Writing – review & editing (equal). **Andreas Fognini**: Funding acquisition (equal); Project administration (lead); Supervision (equal); Writing – review & editing (equal). **Mario U. Castaneda**: Conceptualization (lead); Funding acquisition (lead); Project administration (lead); Resources (lead); Supervision (equal); Writing – review & editing (equal). **Jessica de Wild**: Project administration (equal); Resources (equal); Writing – review & editing (equal). **Bart Vermang**: Resources (equal); Supervision (equal); Writing – review & editing (equal). **Guy Brammertz**: Conceptualization (lead); Funding acquisition (lead); Project administration (lead); Resources (lead); Supervision (equal); Writing – review & editing (equal). **Rainer Erdmann**: Funding acquisition (equal); Project administration (equal); Resources (equal); Supervision (equal).

DATA AVAILABILITY

The data that support the findings of this study are available from the corresponding author upon reasonable request.

REFERENCES

[1] R. Foord, R. Jones, C. J. Oliver, and E. R. Pike, Appl. Opt. **8**, 1975 (1969).

[2] E. Ermilov, C. Oelsner, F. Birke, D. Gerber, V. Buschmann, A. Devaux, and R. Erdmann, Rev. Sci. Instrum. **91**, 069502 (2020).

[3] S. Trautmann, V. Buschmann, S. Orthaus, F. Koberling, U. Ortmann, and R. Erdmann, Application Note on Fluorescence Lifetime Imaging (FLIM) in Confocal Microscopy Applications, PicoQuant, 2012.

[4] C. Kraft, H. Hempel, V. Buschmann, T. Siebert, C. Heisler, W. Wesch, and C. Ronning, J. Appl. Phys. **113**, 124510 (2013).

[5] J. R. Lakowicz, *Principles of Fluorescence Spectroscopy*, 3rd ed. (Springer, New York, 2006).

[6] M. Wahl, Technical Note on Time-Correlated Single Photon Counting, PicoQuant, 2014.

[7] I. Esmaeil Zadeh, J. Chang, J. W. N. Los, S. Gyger, A. W. Elshaari, S. Steinhauer, S. N. Dorenbos, and V. Zwiller, Appl. Phys. Lett. **118**, 190502 (2021).

[8] J. Chang, J. W. N. Los, J. O. Tenorio-Pearl, N. Noordzij, R. Gourgues, A. Guardiani, J. R. Zichi, S. F. Pereira, H. P. Urbach, V. Zwiller, S. N. Dorenbos, and I. Esmaeil Zadeh, APL Photonics **6**, 036114 (2021).

[9] J. Chang, I. E. Zadeh, J. W. N. Los, J. Zichi, A. Fognini, M. Gevers, S. Dorenbos, S. F. Pereira, P. Urbach, and V. Zwiller, Appl. Opt. **58**, 9803 (2019).

[10] I. Esmaeil Zadeh, J. W. N. Los, R. B. M. Gourgues, J. Chang, A. W. Elshaari, J. R. Zichi, Y. J. van Staaden, J. P. E. Swens, N. Kalhor, A. Guardiani, Y. Meng, K. Zou, S. Dobrovolskiy, A. W. Fognini, D. R. Schaart, D. Dalacu, P. J. Poole, M. E. Reimer, X. Hu, S. F. Pereira, V. Zwiller, and S. N. Dorenbos, ACS Photonics **7**, 1780 (2020).

[11] H. Zhang, L. Xiao, B. Luo, J. Guo, L. Zhang, and J. Xie, J. Phys. D: Appl. Phys. **53**, 013001 (2020).

[12] I. Holzman and Y. Ivry, Adv. Quantum Technol. **2**, 1800058 (2019).

[13] See https://www.picoquant.com/products/category/fluorescence-spectrometers/fluotime-250-compact-and-modular-fluorescence-lifetime-spectrometer for the detailed description of the FluoTime 250 spectrometer and its specifications.

[14] See https://singlequantum.com/products/ for detailed description of the Single Quantum Eos SNSPD system.

[15] C. M. Natarajan, M. G. Tanner, and R. H. Hadfield, Supercond. Sci. Technol. **25**, 063001 (2012).

[16] E. A. Dauler, M. E. Grein, A. J. Kerman, F. Marsili, S. Miki, S. W. Nam, M. D. Shaw, H. Terai, V. B. Verma, and T. Yamashita, Opt. Eng. **53**, 081907 (2014).

[17] A. A. Ishchenko, Quantum Electron. **24**, 471 (1994).

[18] M. A. Vasil'eva, V. B. Gul'binas, V. I. Kabelka, A. V. Masalov, and V. P. Syrus, Sov. J. Quantum Electron. **13**, 233 (1983).

[19] J. de Wild, D. G. Buldu, T. Schnabel, M. Simor, T. Kohl, G. Birant, G. Brammertz, M. Meuris, J. Poortmans, and B. Vermang, ACS Appl. Energy Mater. **2**, 6102 (2019).